

Au-Pt-Ni nanochains as dopamine catalysts in neutral media: role of elements and optimization based on spatial distribution

Hua Fan, William Le Boeuf, Vivek Maheshwari*

Supporting Information

1. Cyclic voltammetric (CV) plots at different scan rates

CV plots were recorded from -0.5 to 0.5 V vs. Ag/AgCl at the scan rates of 10 mV/sec, 20 mV/sec, 50 mV/sec, 100 mV/sec, 150 mV/sec, and 200 mV/sec in 0.01 M PBS with 0.5 mM dopamine. As shown in Fig. S1, the CV plots at various scan rates present that the redox peak current increases with the scan rate and redox peaks are assigned to the reversible reaction of dopamine to dopaminoquinone. Furthermore, a linear relationship is observed between the reduction peak potential and the scan rate, v . While the oxidation peak potential varies with $v^{1/2}$. These illustrated that the electrooxidation of dopamine could be a diffusion-controlled process and reduction reaction might be surface adsorption-controlled process.¹

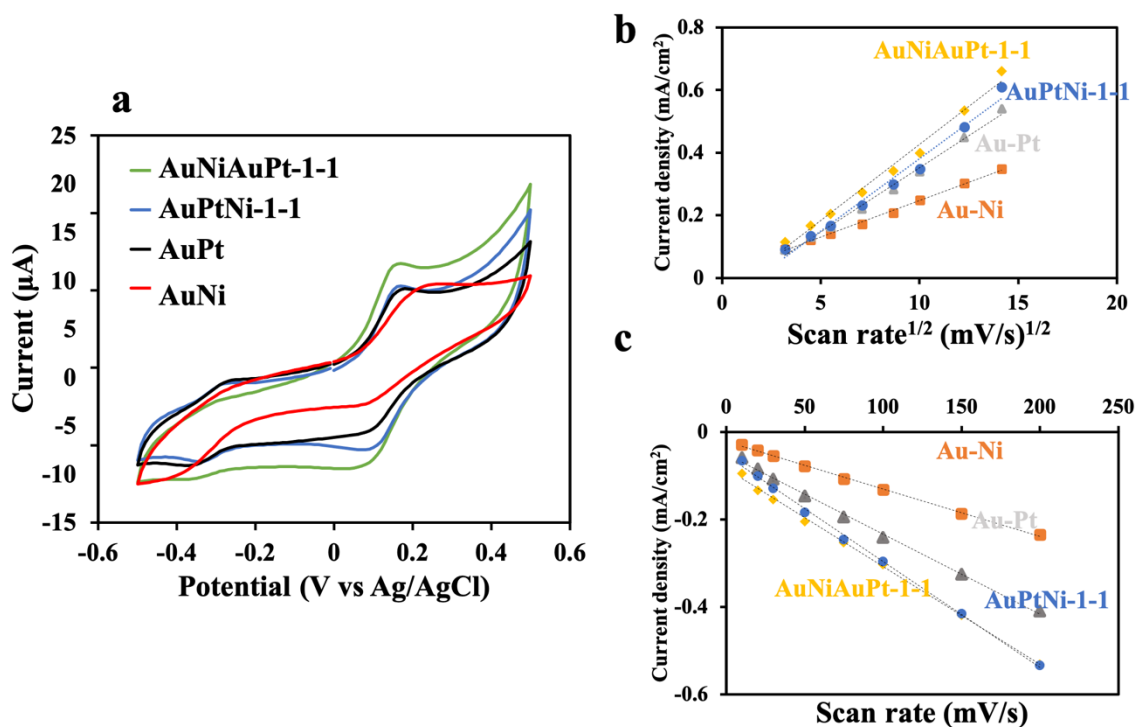


Figure S1. Cyclic voltammograms recorded for Au-Ni, Au-Pt, AuNiAuPt-1-1, and AuPtNi-1-1 samples in PBS with 0.5 mM dopamine; b) Variation of anodic peak currents vs. square root of scan rate and c) variation of cathodic peak currents vs. scan rate in PBS with 0.5 mM dopamine.

2. Effect of deposition mass

To obtain the optimum deposition mass, successive volume addition of the active materials on GCE was investigated in PBS without dopamine. As shown in Fig. S2, a greater amount of the catalyst could increase the current response. In addition, the stacked porous structure can help reactant diffusion to the active sites.² At 15 μL of the sample, maximum current response is observed from the GCE surface, and further addition does not increase the current response. Meanwhile, the material might peel off from the electrode at a higher loading density.³

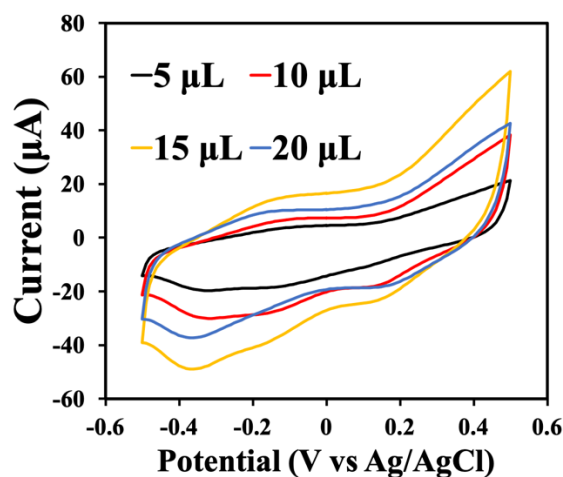


Figure S2. Cyclic voltammograms profile of successive volume addition of the active materials on GCE in PBS.

3. Proposed growth mechanism for the catalyst chains

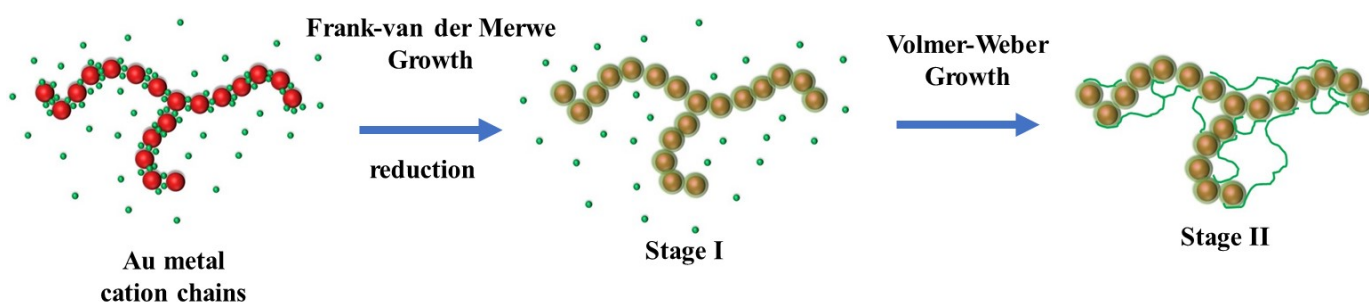


Figure S3. Proposed mechanism for the growth of the catalyst material on the Au chains. The red spheres in first panel are Au nanoparticles, the small green spheres represent the metal cations. In the second panel, a thin shell of the metal/metal oxide is formed on the Au surface. The green shell represents the metal/metal oxide formation around the core of Au nanoparticles. In the last panel small wire/chain like secondary structure are formed from continuing deposition of the metal/metal oxide.

The growth of the Au-Ni-Pt (or Au-Ni-Au-Pt) chains is proposed to be based on a two step process. The first step leads to formation of a uniform layer of the catalyst material on the surface of the Au chains. This occurs as initially a high concentration of the metal cations is present on the surface of the Au nanoparticles, in the electrical double layer (and stern layer) due to strong interaction with the citrate capping of the nanoparticles. On addition of the reducing agent, this high concentration of metal cations leads to formation of a layer of the catalyst material on the Au chains, similar to Frank-van der Merwe growth. Subsequently, the growth of the catalyst layer is sustained by the metal ions in the solution, which do not have a strong interaction with the surface of the chains. The growth hence shifts to Volmer-Weber type process leading to inhomogeneous deposition of the catalyst material (similar to island formation). The TEM images of Fig. 1&5 support this proposed mechanism.

4. Stability of the Au chain catalyst

The Au-Ni-Au-Pt catalyst are tested after storage under ambient conditions for 4 months. The comparison of the performance between a freshly prepared catalyst and after the 4 month storage is shown in Fig. S4. A 7 % drop in sensitivity for dopamine oxidation is observed, which implies that the catalysts are fairly stable.

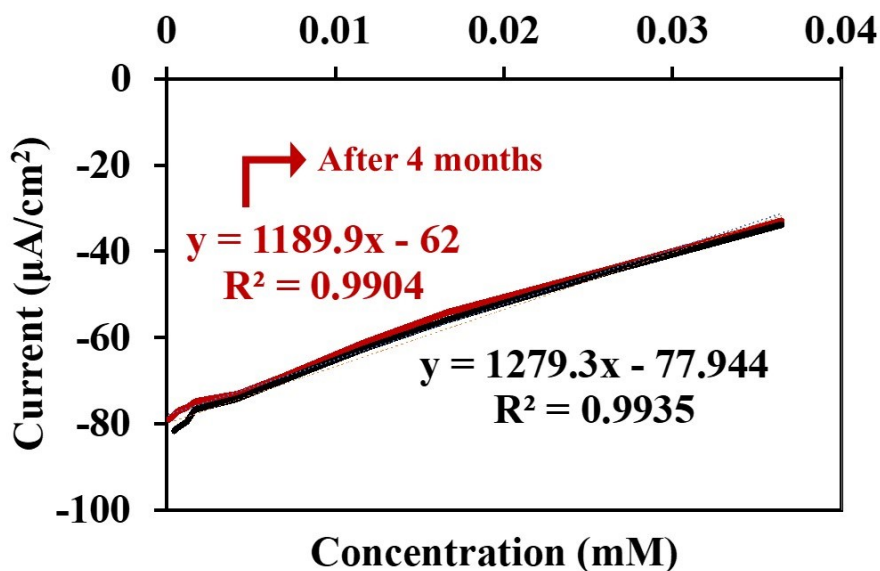


Figure S4. Testing the catalyst performance for dopamine oxidation after storage in ambient conditions for 4 months.

5. Performance comparison between prepared catalyst material in this report and other reports in literature.

Table S5: Comparison of the catalyst performance with literature reports

Sample	Linear range μM	LOD μM	Sensitivity $\mu\text{A mM}^{-1} \text{cm}^{-2}$	Reference
Pt-Ni/PDA/rGO	0.2-911	0.07	912.8	4
GO-AuNCs	1-25	0.028	30.3	5
Au@Pt/GO	0.5-177.5	0.11	329	6
Nafion/Pt/Mesoporous Carbon/GCE	0.1-193	0.034	175	7
Ni(OH) ₂ /NiCo-LDHs	0.05-1080	0.017	83.48	8
Ni(OH) ₂ NBs@CuS NSs HHS	0.02-238	0.003	1011.7	9
Au-Ni-Au-Pt (7:1)	0.19-371.5	0.001	250.8	This work
Au-Pt-Au-Ni (1:1)	0.14-36.5	0.01	1279.3	This work

References

1. N. Elgrishi, K. J. Rountree, B.D. McCarthy, E.S. Rountree, T.T. Eisenhart and J.L. Dempsey. *J. Chem. Educ.*, 2018, **95**, 197-206.
2. M. S. Hsu, Y.L. Chen, C.Y. Lee and H.T. Chiu, *ACS Appl. Mater. Interfaces*, 2012, **4**, 5570-5575.
3. D.W. Hwang, S. Lee, M. Seo and T.D. Chung, *Anal. Chim. Acta*, 2018, **1033**, 1-34.
4. P. Zhao, C. Chen, M. Ni, L. Peng, C. Li, Y. Xie, J. Fei, *Microchimica Acta.*, 2019, **186**, 134.
5. M.K. Alam, M.M Rahman, M.M. Rahman, D. Kim, A.M. Asiri, F. Khan, Feroz, *J. Electroanal. Chem.*, 2019, 835, 329-337.
6. Z. Yang, X. Liu, X. Zheng, J. Zheng, *Electroanal. Chem.*, 2018, 817, 48-54.
7. X. Li, *Int. J Electrochem. Sci.*, 2019, 14, 1082-1091.
8. S. Zhang, Y. Fu, Q. Sheng, J. Zheng, *New J. Chem.*, 2017, 41, 13076-13084.

9. Y. Liu, Y. Liu, H. Ou, D. Shi, L. Tian, Z. Chen, S. Bao, W. Xiao, X. Meng, R. Hu, J. Song, W. Chen, Z. Cheng, G. Zhao, *J. Alloy and Comp.*, 2022, 929, 167390.